Air-Heating Solar Collectors for Humidification-Dehumidification Desalination Systems

Edward K. Summers
e-mail: esummers@mit.edu

John H. Lienhard V[1]
e-mail: lienhard@mit.edu

Department of Mechanical Engineering,
Massachusetts Institute of Technology,
Cambridge, MA 02319-4307 USA

Syed M. Zubair
Department of Mechanical Engineering,
King Fahd University of Petroleum and Minerals,
Dhahran 31261, Saudi Arabia
e-mail: smzubair@kfupm.edu.sa

Relative to solar water heaters, solar air heaters have received relatively little investigation and have resulted in few commercial products. However, in the context of a humidification-dehumidification (HDH) desalination cycle, air heating accounts for advantages in cycle performance. Solar collectors can be over 40% of an air-heated HDH system's cost; thus, design optimization is crucial. Best design practices and sensitivity to material properties for solar air heaters are investigated, and absorber solar absorptivity and glazing transmissivity are found to have the strongest effect on performance. Wind speed is also found to have an impact on performance. Additionally a well designed, and likely low cost, collector includes a double glazing and roughened absorber plates for superior heat transfer to the airstream. A collector in this configuration performs better than current collectors with an efficiency of 58% at a normalized gain of 0.06 K m^2/W.
[DOI: 10.1115/1.4003295]

1 Introduction

Solar water heaters have been thoroughly investigated and developed commercially [1–3], whereas there has been relatively little investigation and almost no commercial development of solar air heaters. These heaters can amount to over 40% of the total cost [4] of a humidification-dehumidification (HDH) system and so the development of a cost effective and efficient solar collector is essential to the system's overall feasibility.

1.1 The Humidification-Dehumidification Cycle. Humidification-dehumidification desalination is a thermal desalination cycle that operates similar to the natural water cycle, where water is evaporated from the oceans by the sun and condenses into fresh water precipitation, which returns to earth and can be used for drinking. This basic principle is behind the operation of a solar still, where the sun evaporates seawater and the vapor condenses on the cooler glazing of the still where it can be recovered for drinking. However, in the process of condensation all the latent heat of evaporation of the water is lost to the environment, leading to poor thermal performance. The HDH cycle improves on this principle by separating the evaporation and condensation processes into different devices thereby recovering the latent heat of evaporation and using it to heat the seawater.

The HDH cycle can be configured in a variety of ways. Figure 1 shows a typical configuration of a HDH cycle. Heating of the air allows greater moisture content by increasing the saturation humidity ratio. However Narayan et al. [5] found that the cycle attains greater thermal performance when the air stream is closed and when the heater is placed after the humidifier, as shown in Fig. 2. It has been found [5] that the cycle performs better using air heating as opposed to water heating. The result is that the heater now has to deal with greater moisture content in the air and has to be robust against corrosion, in addition to being simple and cost effective.

2 Comparing Existing Collectors

Nayaran et al. [6] reviewed potential solar air heaters and compared their efficiency and top temperature output to other collectors in the literature as well as those manufactured commercially. The standard metric of a solar air heater's performance is the collector thermal efficiency. It is defined by Eq. (1).

$$\eta = \frac{\dot{m} c_p (T_{\text{out}} - T_{\text{in}})}{I_T A_p} \tag{1}$$

This definition of performance is that used by the ASHRAE 93-2003 Standard for solar collector testing [7] and it defines both the instantaneous and time averaged efficiencies when evaluating dynamically changing solar radiation inputs and temperature profiles.

In solar collectors, efficiency decreases with fluid temperature gain, as heat losses are directly proportional to temperature. The most common way of showing solar air heater efficiency is to plot the efficiency versus the normalized heat gain as defined by Eq. (2). It has the units K m^2/W.

$$\text{NG} = \frac{(T_{\text{out}} - T_{\text{air}})}{I_T} \tag{2}$$

The normalized gain will decrease with increasing air mass flow rate. Figure 3 [6] shows the reported efficiencies of solar air heaters in the research literature [4,8–19] as a function of normalized heat gain, where better performing heaters are more to the top right portion of the graph, as they deliver the highest air temperature at the highest efficiency. The highest efficiency commercial solar collector, the SunMate Sm-14 [16], is included for comparison. The highest performing heaters are indicated as gray points on the graph, which will set the standard by which new designs will be compared. Of the points indicated in gray, the majority are experimental studies with only one [9] being a theoretical study.

Two outliers [10,12] that do not follow the trend of the other data were excluded from the gray shaded group. Reference [10] is a theoretical study that claims an extremely large efficiency improvement with an addition of porous media as an absorber, with 75% efficiency at 0.12 K m^2/W of normalized gain. However, experiments conducted on a collector in a similar configuration [20] show only 60% efficiency at a normalized gain of 0.017, which is significantly lower. Romdhane [12] provided an experimental study with various types of surface roughening. He reports a near constant efficiency through increasing normalized gain to his highest normalized gain and efficiency. However, when experiments are done by varying the mass flow rate, the same collector shows a linearly increasing trend with increasing mass flow

[1]Corresponding author.

Contributed by the Solar Energy Division of ASME for publication in the JOURNAL OF SOLAR ENERGY ENGINEERING. Manuscript received May 16, 2010; final manuscript received October 27, 2010; published online February 14, 2011. Assoc. Editor: Gregor P. Henze.

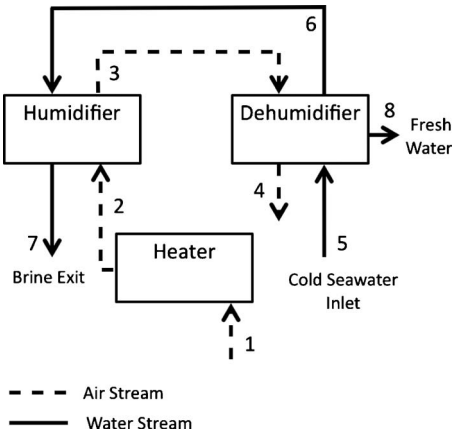

Fig. 1 A typical air-heated HDH cycle

rate, which is expected. The increase in mass flow rate is accompanied by a decrease in temperature rise (and normalized gain) as the air has a shorter residence time in the collector. This appears to be inconsistent with the reported results for varying normalized gain. By comparing the designs of the five best heaters, a list of apparent best design practices can be obtained.

Air flow over the absorber plate. Having air flow above the absorber decreases losses from the top of the absorber plate and eliminates conduction resistance through the plate. Many modern air heaters use this method [8,9,17].

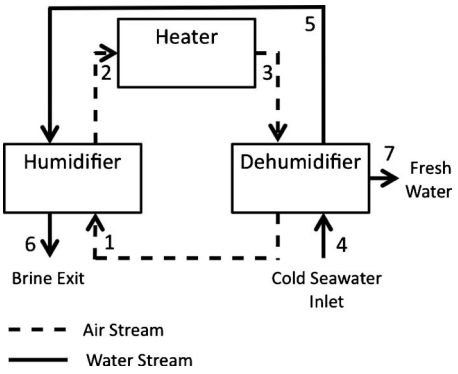

Fig. 2 A closed air HDH cycle as developed by Narayan et al. [5]

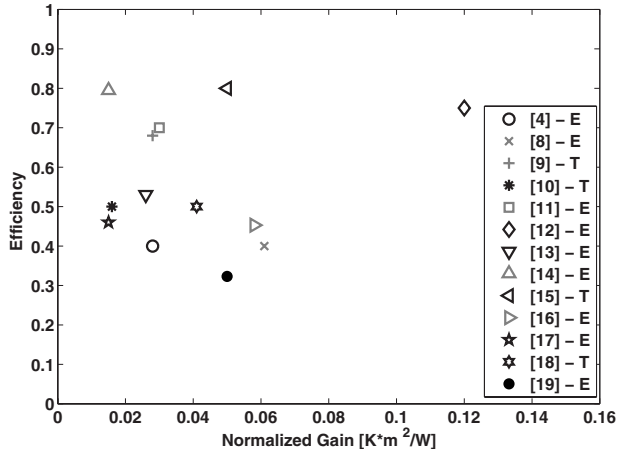

Fig. 3 Normalized comparison of solar air heaters in literature. "E" denotes an experimental study and "T" denotes a theoretical study [6].

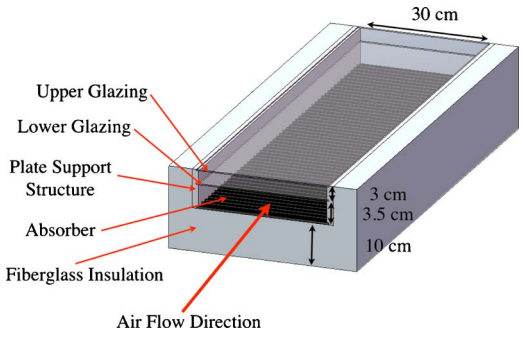

Fig. 4 Diagram of heater cross-section

Packing materials. Packing materials in the air stream improve heat transfer by mixing the air and providing more surface area to absorb radiation. Packing also provides sensible heat storage but comes at the cost of high pressure drop [9,13]. In the context of HDH, the materials have to be moisture and corrosion resistant. Since they add effective energy storage to the collector, they will be considered in a separate study of transient solar collector designs.

Roughened absorber plate. A roughened absorber plate improves convection heat transfer into the air. A rough configuration also increases pressure drop, but only marginally when compared with a smooth plate for duct cross-sections used in solar air heating. Roughening for increased convection has been extensively investigated and has shown performance improvements in collectors [10,17].

Multiple passes of air through the collector. Multiple passes of air through the collector improves heat gain by increasing contact with the absorber and makes the absorber run cooler, decreasing losses [13]. However the same can be accomplished with a rough absorber plate without having a very thermally conductive absorber. This allows many more materials to be used as absorber surfaces, such as those with low thermal conductivity.

Multiple glazing layers. Multiple glazing layers reduce heat loss by infrared radiation and trap an insulating air layer between the glazings. However, this comes at a greater material cost and lower solar transmissivity. All of the top performing heaters except those used by Sahu and Bhagoria [17] use a double glazing.

Glass and metal construction. Glass and metal construction provides better heat transfer characteristics and better durability. All the best performing collectors used glass and metal construction, as polymer alternatives, especially for glazings, suffer from low durability, although initially providing optical properties comparable to glass [21].

3 Sensitivity of Heater Performance to Material Properties and Environmental Conditions

3.1 Baseline Design. Using information gleaned from the literature review, a simple baseline design was devised. To obtain the required temperature rise, a long and narrow collector was necessary, and it has a cross-section as illustrated in Fig. 4. In reality, this long effective collector can be achieved by placing shorter modules in series. The total length of the collector is 10 m, and it consists of an aluminum absorber coated with carbon black paint, and low-iron glass glazing panels. The outside is insulated with fiberglass insulation. The outdoor wind speed is assumed to be a moderate 5 m/s, which is consistent with averages for a desert climate like the one found in Saudi Arabia [22]. The characteristic length over which wind blows is the average of the width and length of the collector as wind direction is highly variable. The absorber is roughened with transverse ribs to increase turbulence and heat transfer. The ribs have a constant height and pitch throughout the channel. Tables 1 and 2 outline the fixed parameters of the baseline design. The dimensions of the flow

Table 1 Constant parameters for simulating baseline design

Constants	Values
Solar irradiation	900 W/m^2
Ambient wind speed	5 m/s
Latitude	27 deg
Solar declination	23 deg
Collector tilt angle	45 deg
Collector inlet temperature	30°C
Ambient air temperature	30°C
Dew point temperature	4°C
Insulation conductivity	0.02 W/m K

channel were chosen so that all analysis occurs in the turbulent flow regime. The analysis only varies one of the material properties in Table 2 at a time, keeping all the others constant.

3.2 Governing Equations. In steady state, the heat transfer processes in the collector can be modeled as a series of thermal resistances. They are shown in Fig. 5. If control volumes are taken around the two glazings, the absorber and the air stream, and the heat flows between each of the control volumes are balanced, Eqs. (3) are obtained.

$$U_t(T_{\text{amb}} - \bar{T}_{c1}) + h_r(\bar{T}_a - \bar{T}_{c1}) + h_2(\bar{T}_f - \bar{T}_{c1}) = 0 \quad (3a)$$

$$S + U_b(T_{\text{amb}} - \bar{T}_a) + h_r(\bar{T}_{c1} - \bar{T}_a) + h_1(\bar{T}_f - \bar{T}_a) = 0 \quad (3b)$$

$$h_2(\bar{T}_{c1} - \bar{T}_f) + h_1(\bar{T}_a - \bar{T}_f) = q_u \quad (3c)$$

where terms are defined in the Nomenclature. S is defined by multiplying the irradiation I by $(\tau\alpha)$, which is the combined solar transmissivity and absorptivity of the absorber and cover system. S is calculated from optical properties and geometry using equations from Duffie and Beckman [21]. The above equations can be solved for the fluid temperature and integrated along the length of the collector. However, in steady state, where heat capacity can be neglected, the integrated differential equation can be expressed explicitly using several lumped parameters as recommended by Duffie and Beckman [21]. Figure 5 shows radiation to the same ambient air temperature as convection, which is required for the use of simple lumped parameters. Duffie and Beckman [21] state that sky temperature is relatively unimportant for calculating collector performance. However, this may become important as the collector is required to run hotter and radiative loss is more important. Therefore, sky temperature is included in these calculations and T_{amb} is defined as a sol-air temperature of the environment by Eq. (4). A correlation [21] for sky temperature based on dew point temperature is used. The sol-air temperature is used for the total loss despite the fact that there is no radiation from the back surface to the sky. This does not have a large effect on the loss, as the bottom loss is only 3% of total loss in the baseline configuration.

Table 2 Baseline values of varied material properties

Material properties	Value
Glazing refraction index	1.526
Glazing extinction coefficient	4
Absorber solar absorptivity	0.94
Glazing IR emissivity	0.92
Absorber IR emissivity	0.86
Transmittance absorptance product-$(\tau\alpha)$	0.77

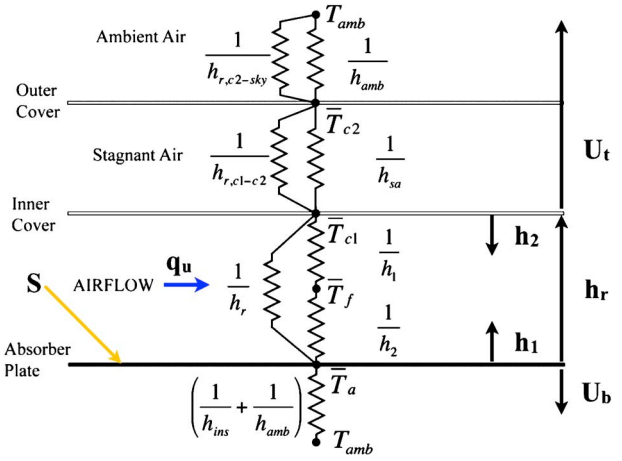

Fig. 5 Heat transfer resistances with lumped parameters

Table 3 Roughening parameters

Roughening parameters	Value
Rib height, h	0.0032 m
Rib pitch, p	0.02 m
p/h	6.3
Roughening regime	Fully rough

Heat transfer coefficients are calculated using commonly used correlations for natural and forced convection heat transfer [23]. Radiation heat transfer coefficients are linearized radiation heat transfer expressions in the form of $h_{\text{rad}}=4\sigma\bar{T}^3\mathcal{F}_{1-2}$, as given by Lienhard and Lienhard [24]. The surface was modeled as having transverse rib roughening using the equations developed by Dalle Donne and Meyer [25]. The roughening parameters are given in Table 3.

Since the glazings are made of glass, they are assumed to be opaque in the infrared. Polymeric glazings that may be beneficial for cost and thermal performance are not always opaque in the infrared and allow some reradiative loss. In addition, polymeric glazings may be very thin and thus hard to clean or susceptible to damage by UV radiation and blown sand; and they will not be considered here.

Equation (5) is a combined loss coefficient resulting from algebraic manipulations of Eq. (3).

$$U_L = \frac{(U_t + U_b)(h_1h_2 + h_1h_r + h_2h_r) + U_bU_t(h_1 + h_2)}{h_1h_r + h_2U_t + h_2h_r + h_1h_2} \quad (5)$$

With a combined loss coefficient, a simple energy balance leads to Eq. (6)

$$q_u = [S - U_L(\bar{T}_a - T_{\text{amb}})] \quad (6)$$

where q_u is useful heat gained by the air. Since the mean plate temperature is unknown, it needs to be found iteratively. Equation (7) gives the integrated solution in terms of a heat removal factor and loss factor given by Eq. (8).

$$\bar{T}_a = T_{\text{amb}} + \frac{q_u}{F_RU_L}(1 - F_R) \quad (7)$$

$$F_R = \frac{\dot{m}c_p}{A_pU_L}\left[1 - \exp\left(\frac{-A_pU_LF'}{\dot{m}c_p}\right)\right] \quad (8a)$$

$$F' = \frac{h_rh_1 + h_2U_t + h_2h_r + h_1h_2}{(U_t + h_r + h_1)(U_b + h_r + h_2) - h_r^2} \quad (8b)$$

$$T_{\text{amb}} = T_{\text{air}} + \frac{-h_{\text{rad},c2-\text{sky}}(T_{\text{air}} - T_{\text{sky}})}{h_{\text{amb}} + h_{\text{rad},c2-\text{sky}}} \quad (4)$$

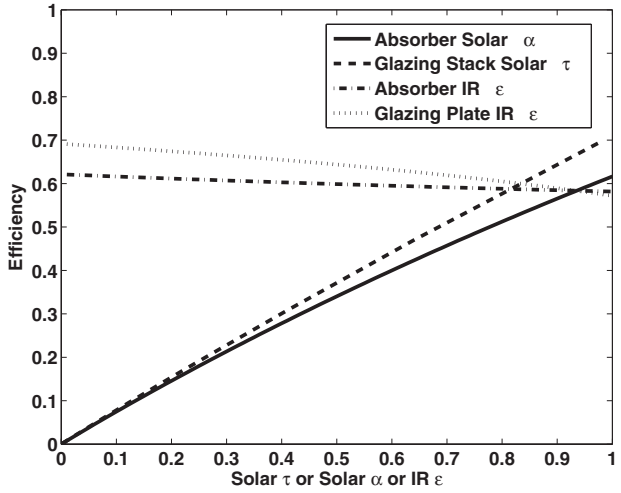

Fig. 6 Effect of emissivity, absorber absorptivity, and glazing transmissivity on collector efficiency

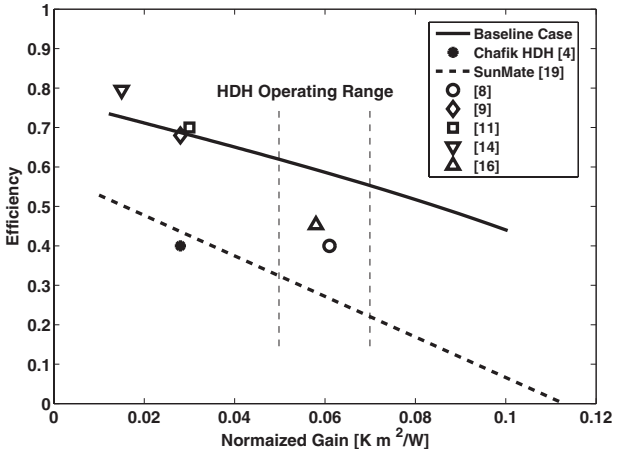

Fig. 7 Effect of design enhancements on collector performance

At each iteration all temperatures and individual heat transfer coefficients that make up lumped parameters, such as U_t, are recalculated. Since all heat transfer coefficients are linearized, calculating an energy balance based on the lumped parameters used in Eq. (3) is equivalent to taking all regions separately and using individual heat transfer coefficients.

After convergence the final plate temperature is used in Eq. (6) and the useful heat is divided by the total solar irradiation to obtain an efficiency. The air temperature rise is given by dividing the useful heat by the capacity rate of the air, $\dot{m}c_p$. To characterize how the efficiency behaves versus the temperature rise in the collector, an equivalent effectiveness [21] is defined by Eq. (9).

$$F_O = \frac{\frac{\dot{m}c_p}{A_p U_L}\left[1 - \exp\left(\frac{-A_p U_L F'}{\dot{m}c_p}\right)\right]}{\exp\left(\frac{-A_p U_L F'}{\dot{m}c_p}\right)} \tag{9}$$

The efficiency versus normalized gain curve takes the form of Eq. (10).

$$\eta = F_O(\tau\alpha) - F_O U_L\left[\frac{T_{\text{out}} - T_{\text{amb}}}{I_T}\right] \tag{10}$$

The normalized gain in Eq. (10) is different from Eq. (2) in that it is based on the outlet and ambient temperature difference. However, since the calculations on the baseline collector were done by fixing the air inlet T_{in} to T_{amb} this equation can describe the efficiency versus normalized gain with normalized gain as it is defined in Eq. (2). F_O is analogous to a heat exchanger effectiveness. Therefore, the collector performs better at higher normalized gain if it has high glazing transmissivity and absorber absorptivity of solar radiation, if losses are minimized, and if the heat transfer coefficient from the absorber to the air is high.

3.3 Sensitivity Analysis Results. A sensitivity study investigated the effect of various material properties on performance of the collector, as well as how environmental conditions affect the performance when certain materials are used.

3.4 Material Properties. The material properties that have the greatest impact on performance are the infrared emissivities of the glazing and absorber plates, the glazing stack solar transmissivity, and absorber solar absorptivity. Figure 6 shows the relative effect of each parameter as it is varied from 0 to 1. The operating point was based on the operation of a HDH cycle in a desert environment. For the 10 m long collector, a normalized gain of 0.06 K m^2/W is obtained at a mass flow rate of 0.029 kg/s. The calculations assume that the conduction resistances of the glazings and absorber are negligible, owing to their small thickness. Heater dimensions can be optimized for the desired temperature rise, and optima are easily found for the dimensions of roughness features or spacing between the plates and will not be discussed here. The graph shows that the two most important parameters are absorber solar absorptivity and glazing solar transmissivity. Using an absorber with a selective coating (α=0.9–1, ε=0.02–0.3) [26] does not offer significant performance gains with only 4% efficiency improvement. This can be an expensive design addition, as selective surfaces often made of somewhat exotic materials, such as quartz, can involve expensive manufacturing processes and are limited to only a few substrates. Using a low ε coating for the glazing plates offers a larger improvement of 10%, but also can be an expensive addition.

To ascertain the efficiency "value" of various design attributes, heaters were simulated in different configurations, adding various design improvements onto a collector with a smooth, nonselective absorber with a single glazing. As can be seen from Fig. 7, the addition of surface roughness increases performance by the greatest amount in the HDH operating range. A typical value for a fully roughened surface using the parameters in Table 3 can increase the heat transfer coefficient 8 times over that for a smooth plate. The use of a selective absorber coating (ε=0.05) also improves performance by a small amount. For low normalized gain, a selective surface does not improve performance for over a roughened absorber, although it is more important at higher temperatures where radiative losses dominate. Figure 8 shows how the baseline design compares with existing air heaters that include Chafik's HDH collector [4] and the SunMate commercial collector [16] for which the performance curve is available. It is clearly shown that the baseline collector, which incorporates all of the design enhancements beside a selective absorber, outperforms existing collectors in the HDH operating range.

3.5 Environmental Conditions. Environmental conditions also influence how a collector can be designed and the importance of design enhancements. The environmental parameters of most importance are the ambient air temperature, the dew point temperature, which affects sky temperature, and ambient wind speed. As suggested in the literature [21] ambient air temperature has a small effect on performance when compared with ambient wind speed. A variation in dew point temperature from −4 °C to 36 °C translates into a 1–2% efficiency change in the HDH operating range, and a change in ambient air temperature from 0 °C to 40 °C translates into a 3–4% efficiency change in the HDH operating range.

Wind speed has a larger effect on performance. Figure 9 shows

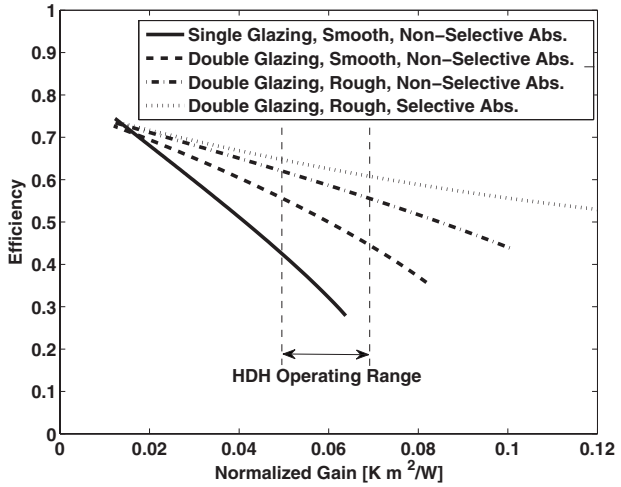

Fig. 8 Comparison of baseline design (double glazed, rough, nonselective absorber) with existing air heaters

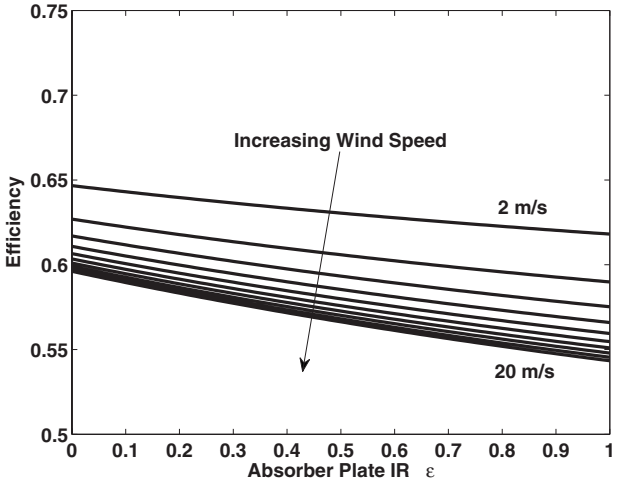

Fig. 10 Effect of wind speed on collector performance at different absorber IR emissivity

that wind speed can have a substantial effect on performance in the HDH operating range, with an efficiency change of 10–12%. Figures 10 and 11 show the effect of wind speed on performance at varying infrared emissivities for glazing and absorber plates. The lines each represent a different wind speed from 2 m/s (h_{amb}=3.07 W/m^2 K) to 20 m/s (h_{amb}=39.74 W/m^2 K) in increments of 2 m/s. The graphs show that using low ε surfaces is of low importance in calm environments with only marginal improvement in windy ones.

4 Conclusion

Air heating solar collectors have been studied for conditions typical of a HDH desalination system. Overall, improving the transmissivity of the glazing by using highly transmissive polymer films or low iron glass, and using a very absorptive absorber, which is inexpensively accomplished by including a carbon black coating, would have the largest impact on performance. The greatest improvement to a collector's performance can be accomplished by using a double glazing, resulting in a 20% efficiency increase in the HDH operating range compared with a single glazed collector. This reduces radiative losses as glass is opaque to infrared radiation. An insulating layer of trapped air between the plates also lowers the outer collector temperature and further decreases convective and radiative losses. The second most important enhancement is the addition of a rough surface on the absorber plate, which improves convection from the heat source to the air. This offers up to 12% efficiency increase without the need for a selective surface on the absorber. Adding a selective surface to the absorber, or a low emissivity coating to the glazing, can add cost as a result of the use of exotic materials. In the HDH operating range these improvements have limited impact on performance, even when environmental conditions change adversely. Of the environmental conditions that affect performance, wind speed has the greatest impact. The wind speed increases the already dominant convective losses from the collector. A collector with a double glazing, a highly roughened absorber, and a carbon black coated absorber, results in a collector efficiency of 58% at a normalized gain of 0.06 K m^2/W. This offers significant performance gains over existing solar air heaters, which is accomplished in a simple and possibly inexpensive design.

Acknowledgment

The authors would like to thank the King Fahd University of Petroleum and Minerals for funding the research reported in this paper through the Center for Clean Water and Clean Energy at MIT and KFUPM. The authors are grateful to P. Gandhidasan and M.A. Antar for useful discussions of this work.

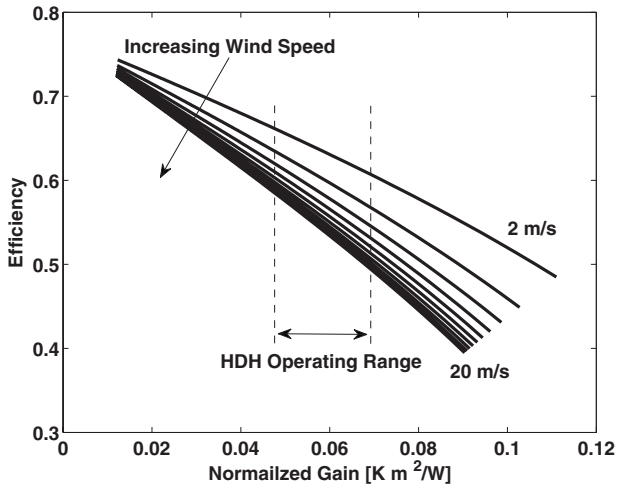

Fig. 9 Collector efficiency vs normalized gain for different wind speeds

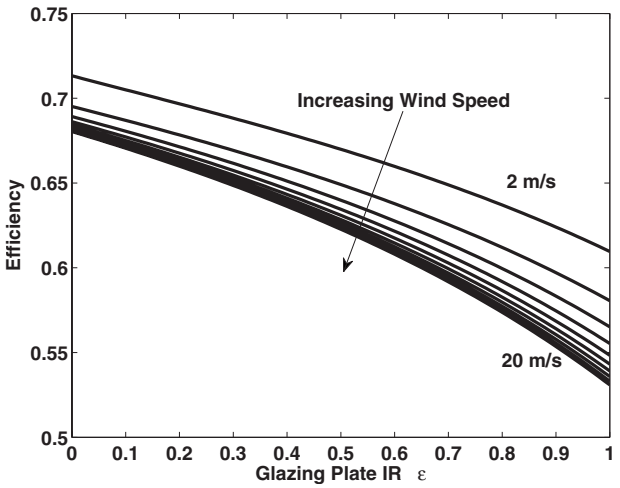

Fig. 11 Effect of wind speed on collector performance at different glazing IR emissivity

Nomenclature

Roman Symbols

A_p = collector area, m^2
c_p = specific heat capacity of air at constant pressure, J/kg K
$\mathcal{F}_{1-2}$ = radiation transfer factor
F' = heat gain factor
F_O = equivalent effectiveness
F_R = heat removal factor
h = average convective heat transfer coefficient, W/m^2 K
h_1 = absorber to fluid convective heat transfer coefficient, W/m^2 K
h_2 = inner glazing to fluid convective heat transfer coefficient, W/m^2 K
h_{amb} = convective heat transfer coefficient to ambient air, W/m^2 K
h_{ins} = bottom insulating layer heat transfer coefficient, W/m^2 K
h_r = absorber to glazing radiative heat transfer coefficient, W/m^2 K
$h_{r,c1-c2}$ = radiation heat transfer coefficient, between glazing layers, W/m^2 K
$h_{r,c2-sky}$ = radiation heat transfer coefficient, outer glazing to sky, W/m^2 K
h_{sa} = interglazing natural convection heat transfer coefficient, W/m^2 K
I_T = solar irradiation, W/m^2
$\dot{m}$ = mass flow rate of air through the collector, kg/s
NG = normalized gain, K m^2/W
q_u = useful heat gain by the fluid per unit collector area, W/m^2
S = solar flux absorbed by the absorber, W/m^2
T = temperature, K
$\bar{T}$ = mean temperature, K
U_b = overall bottom loss heat transfer coefficient, W/m^2 K
U_L = overall heat loss coefficient, W/m^2 K
U_t = overall top loss heat transfer coefficient, W/m^2 K

Greek Symbols

α = solar absorptivity
ε = infrared emissivity
η = collector efficiency
τ = solar transmissivity
$(\tau\alpha)$ = solar transmittance absorptance product

Subscripts

a = absorber
air = ambient air
amb = sol-air
$c1$ = inner glazing
$c2$ = outer glazing
f = fluid or air stream
in = air inlet
out = air outlet
sky = sky

References

[1] Eggers-Lura, A., 1978, *Solar Energy for Domestic Heating and Cooling: A Bibliography With Abstracts, and a Survey of Literature and Information Sources*, Pergamon, New York.
[2] Garg, H., 1985, "Solar Water Heating Systems," Proceedings of the Workshop on Solar Water Heating Systems, Dordrecht.
[3] Kalogirou, S. A., 2004, "Solar Thermal Collectors and Applications," Prog. Energy Combust. Sci., **30**, pp. 231–295.
[4] Chafik, E., 2002, "A New Type of Seawater Desalination Plants Using Solar Energy," Desalination, **1**(153), pp. 25–37.
[5] Narayan, G. P., Sharqawy, M. H., Lienhard V, J. H., and Zubair, S. M., 2010, "Thermodynamic Analysis of Humidification-Dehumidification Desalination Cycles," Desalination and Water Treatment, **16**(1), pp. 339–353.
[6] Narayan, G. P., Sharqawy, M. H., Summers, E. K., Lienhard V, J. H., Zubair, S. M., and Antar, M. A., 2010, "The Potential of Solar-Driven Humidication-Dehumidication Desalination for Small-Scale Decentralized Water Production," Renewable Sustainable Energy Rev., **14**(4), pp. 1187–1201.
[7] Rojas, D., Beermann, J., Klein, S. A., and Reindl, D. T., 2008, "Thermal Performance Testing of Flat-Plate Collectors," Sol. Energy, **82**(8), pp. 746–757.
[8] Satcunanathan, S., and Deonarine, S., 1973, "A Two-Pass Solar Air Heater," Sol. Energy, **15**(1), pp. 41–49.
[9] Mittal, M., and Varshney, L., 2006, "Optimal Thermohydraulic Performance of a Wire Mesh Packed Solar Air Heater," Sol. Energy, **80**(9), pp. 1112–1120.
[10] Mohamad, A., 1997, "High Efficiency Solar Air Heater," Sol. Energy, **60**(2), pp. 71–76.
[11] Esen, H., 2008, "Experimental Energy and Exergy Analysis of a Double-Flow Solar Air Heater Having Different Obstacles on Absorber Plates," Build. Environ., **43**(6), pp. 1046–1054.
[12] Romdhane, B. S., 2007, "The Air Solar Collectors: Comparative Study, Introduction of Baffles to Favor The Heat Transfer," Sol. Energy, **81**(1), pp. 139–149.
[13] Ramadan, M., El-Sebaii, A., Aboul-Enein, S., and El-Bialy, E., 2007, "Thermal Performance of a Packed Bed Double-Pass Solar Air Heater," Energy, **32**(8), pp. 1524–1535.
[14] Koyuncu, T., 2006, "Performance of Various Design of Solar Air Heaters for Crop Drying Applications," Renewable Energy, **31**(7), pp. 1073–1088.
[15] Matrawy, K. K., 1998, "Theoretical Analysis for an Air Heater With a Box-Type Absorber," Sol. Energy, **63**(3), pp. 191–198.
[16] Solar Rating and Certification Corporation, 2008, Directory of Certified Solar Collector Ratings.
[17] Sahu, M., and Bhagoria, J., 2005, "Augmentation of Heat Transfer Coefficient by Using 90 Degree Broken Transverse Ribs on Absorber Plate of Solar Air Heater," Renewable Energy, **30**(13), pp. 2057–2073.
[18] Close, D. J., 1963, "Solar Air Heaters for Low and Moderate Temperature Applications," Sol. Energy, **7**(3), pp. 117–124.
[19] Sharma, V. K., Sharma, S., Mahajan, R. B., and Garg, H. P., 1990, "Evaluation of a Matrix Solar Air Heater," Energy Convers. Manage., **30**(1), pp. 1–8.
[20] Sopian, K., Alghoul, M., Alfegi, E. M., Sulaiman, M., and Musa, E., 2009, "Evaluation of Thermal Efficiency of Double-Pass Solar Collector With Porous-Nonporous Media," Renewable Energy, **34**(3), pp. 640–645.
[21] Duffie, J. A., and Beckman, W. A., 2006, *Solar Engineering of Thermal Processes*, 3rd ed., Wiley, Hoboken, NJ.
[22] Elhadidy, M., and Shaahid, S., 2007, "Wind Resource Assessment of Eastern Coastal Region of Saudi Arabia," Desalination, **209**(1–3), pp. 199–208.
[23] Mills, A. F., 1992, *Heat and Mass Transfer*, 2nd ed., Irwin, Boston, MA.
[24] Lienhard V, J. H., and Lienhard, J. H., IV, 2006, *A Heat Transfer Textbook*, 3rd ed., Phlogiston, Cambridge, MA.
[25] Dalle Donne, M., and Meyer, L., 1977, "Turbulent convective Heat Transfer From Rough Surfaces With Two-Dimensional Rectangular Ribs," Int. J. Heat Mass Transfer, **20**, pp. 583–620.
[26] Kennedy, C., 2002, "Review of Mid-to High-Temperature Solar Selective Absorber Materials," Technical report, National Renewable Energy Laboratory.